J Mol Model (2014) 20:2455
DOI 10.1007/s00894-014-2455-6

ORIGINAL PAPER

Bonding analysis of the donor–acceptor sandwiches CpE–MCp (E = B, Al, Ga; M = Li, Na, K; Cp = η^5-C_5H_5)

Suhong Huo · Decheng Meng · Xiayan Zhang · Lingpeng Meng · Xiaoyan Li

Received: 7 June 2014 / Accepted: 1 September 2014 / Published online: 17 September 2014

Abstract The nature of E–M bonds in CpE–MCp (E = B, Al, Ga; M = Li, Na, K; Cp = η^5-C_5H_5) donor–acceptor sandwiches was studied using the atoms in molecules (AIM) theory, electron localization function (ELF), energy decomposition analysis (EDA), and natural bond orbital analysis (NBO) methods. Both topological and orbital analysis show that the E atom determines the bond strength of the E–M bonds, while the M atom has little influence on it. E–M bond strength decreases in the order E = B, Al, and Ga. The EDA analysis shows that the electrostatic character decreases following the sequence E = B > Al > Ga. Not only the *s* orbital, but also the *p* orbital of the E/M atom participates in formation of the E–M bond. The interactions of E and M with Cp are different. The M–Cp interaction is purely electrostatic while the E–Cp interaction has a partly covalent character.

Keywords Donor–acceptor sandwich · E–M bonds · Atoms in molecules · Electron localization function · Energy decomposition analysis

Introduction

The chemistry of metallocenes continues to attract a great deal of attention [1, 2] due to their successful application in many areas of chemistry, such as olefin polymerization catalysis [3], asymmetric catalysis [4], C–H bond activation [5] and bio-organometallic chemistry [6]. A recent breakthrough in organometallic chemistry has been the synthesis in 2004 of decamethyldizincocene Cp*Zn–ZnCp* (Cp*=η^5-C_5Me_5) [7]. In this remarkable D_{5h}-symmetry compound, a pair of metal atoms is sandwiched between two Cp* rings. This discovery triggered the interest of several groups in carrying out further study of bis-metallic sandwiches [8–12]. Recently, Timoshkin and Schaefer [13] reported a series of novel main group heterodinuclear metallocenes formed by donor–acceptor interactions of CpE and CpM (E = B, Al, Ga; M = Li, Na, K). E element compounds, in oxidation state +1, possess a lone pair, while the M element complex, in oxidation state +1, has a vacant orbital. Therefore, the formation of CpE–MCp would be formally achieved by a donor–acceptor interaction between the half-sandwich CpE and CpM. This was the first introduction of the donor–acceptor interaction concept to dinuclear metallocenes. Roesky's group [14] synthesized the compound CpLn–AlCp (Ln = Eu, Yb) in moderate yield. Furthermore, Merino et al. [15] designed a series of structures with the general formula CpM'–MPyl (M' = B, Al, Ga; M = Li, Na; Pyl = η-C_5H_7) by means of density functional theory (DFT), and He et al. [16] predicted the stability of CpM'–MCp for M' = B, Al, Ga, In, Tl and M = Li, Na, K.

All of these reports agreed that the CpE–MCp (E = B, Al, Ga; M = Li, Na, K) sandwiches were stable, and CpE and MCp were connected by a donor–acceptor interaction, from the point of view of molecular orbital theory. However, when the E and M elements are both in oxidation state +1, it is difficult to understand how the E element interacts with M. The E–M bond lengths calculated by Timoshkin and Schaefer [13] and He et al. [16] are similar; they are much larger than the sum of the ionic radii of E and M but smaller than Pauling's single-bond metal radius [17]. The question becomes, what kind of interaction existing between the E and M atom should then be investigated. Both the origin and the

S. Huo · D. Meng · X. Zhang · L. Meng · X. Li (✉)
College of Chemistry and Material Science, Hebei Normal University, Road East of 2nd Ring South, Shijiazhuang 050024, China
e-mail: lixiaoyan326@163.com

S. Huo
College of Chemical and Materials Engineering, Yanching Institute of Technology, Road North of Yingbin, Yanjiao National High-tech Industry Development Zone, 101601 Sanhe, China

nature of the E–M bond are worthy of notice. Recently, two different theoretical approaches, namely the 'atoms in molecules' (AIM) [18, 19] and the electron localization function (ELF) [20–23] methods have become increasingly popular. Both can provide accurate definition of the chemical concepts of the chemical bond. The energy decomposition analysis (EDA) method developed by Morokuma [24] and Ziegler and Rauk [25] is very helpful for the quantitative analyses of chemical bonding. Therefore, one can expect that these methodologies will provide further insight into the nature of the chemical bonding in these remarkable compounds.

The goal of this work was to gain deeper insight into the bonding characteristics of the dinuclear metallocenes CpE–MCp. The scope of this paper is two-fold. Firstly, the E–M bonds were investigated using AIM and ELF techniques. The nature of E–M bonds is discussed based on the properties of the bond critical point (BCP) and valence basins. Secondly, an EDA of the CpE–MCp bond was carried out. This gives the components of the bond dissociation energies that are associated with the E–M bond. Our studies are also expected to provide useful information for additional chemical syntheses and to stimulate further studies of the dinuclear metallocenes.

Computational methods

The hybrid density functional B3LYP has proven to be an accurate method for sandwich complexes [26]. The DFT (B3LYP) [27, 28] calculations were carried out with the Gaussian 03 package of programs [29] using the 6−311++G(d, p) [30, 31] basis set. Vibrational analysis was used to check the nature of the stationary points at the same level. The bond characteristics of the compounds were analyzed using the AIM [18, 19, 32] theory of Bader, and carried out using the AIM2000 [33] and AIMALL [34] programs. The ELF were plotted and analyzed using TopMod [35–37] and multiwfn [38] software. The delocalization index (*DI*) was calculated at B3LYP/6−311++G(d, p) level using a Hartree-Fock (HF)-like electron-pair density. For all other topological studies, the wave functions were calculated at the B3LYP/6−311++G(d, p) level. The decomposition of interaction energies was carried out using the ADF2008.1 program [39] calculated at the BLYP/TZP level. Scalar approximation relativistic effects were accounted for using the zeroth-order regular approximation (ZORA) [40]. The NBO analysis was carried out using the NBO package included in the Gaussian 03 suite of programs [41, 42].

Results and discussion

The optimized geometries of CpE–MCp are shown in Fig. 1, and their structural parameters are given in Table 1. All of the compounds have C_{5v} symmetry, where the centers of the two η^5-C_5H_5 groups and the E and M atoms are collinear. The calculated geometries are very close to the results of Timoshkin and Schaefer [13] and He et al. [16], which were obtained at the B3LYP/TZVP and B3LYP/6−311+G(d, p) levels.

AIM analysis

The AIM method [18, 19, 32] has proved to be a powerful theory for the exploration and characterization of chemical bonds. According to AIM theory, chemical bonding is identified by a (3, −1) critical point (CP) between maxima, the presence of which is a necessary and sufficient condition for atoms to be bonded to one another [18]. The characterization of the electron density and derived properties at these (3, −1) CPs provide valuable descriptions of the chemical bonding. In order to discuss the nature of the E–M bonding, AIM analysis was performed. The molecular graphs of CpEMCp are also shown in Fig. 1 and the topological properties at the BCPs are listed in Table 2.

As shown in Fig. 1, there is a BCP between the E and M atoms and there is one bond path linking the BCP to the E and M atoms. This provides a universal indicator of the bonding that exists between the linked atoms. Generally speaking, the electron density $\rho(r_c)$ at the BCP reliably reflects the strength. The larger the value of ρ_c, the stronger the interaction [32]. As can be seen from Table 2, for the same E atom, the values of $\rho(r_c)$ at the BCP of the E–M bond decrease in the order M = Li > Na > K. For the same M atom, $\rho(r_c)$ at the BCP of the E–M bond decreases in the order E = B > Al > Ga. The *DI* values show the same trend. The *DI* is associated with the covalent bond order [43], and can be used to estimate the formal bond order of a chemical bond in an alternative way; only approximate *DI*s are obtained at the DFT level, whatever the functional used [44–46]. The $\rho(r_c)$ at the BCP show that the E–M strength decreases in the sequence E = B > Al> Ga. For all of the studied compounds, the Laplacians of the density, $\nabla^2\rho(r_c)$, at the BCP of the E–M bond are positive and the $-G_c/V_c$ values are larger than 1.0. According to Cremers' criteria [47, 48], the E–M bonds display the characteristic of "closed shell" ionic interactions.

As for the metal–ligand interactions, there are five BCPs between the E/M atoms and the carbon atoms of the C_5H_5 ring. The topological parameters of these five BCP are exactly the same. In complexes, the $\rho(r_c)$ at the BCP of the M–C (M = Li, Na, K) bond increases in the sequence B < Al < Ga. Comparing to the topological parameters of the BCP of M–C and E–C before complexation, the $\rho(r_c)$ at the BCP of the M–C bond decreases while that at the BCP of the E–C (E = B, Al, Ga) bond increases. The $\rho(r_c)$ change tendencies at the BCPs of the E–C and M–C bond mean that the formation of E–M bonds strengthens the E–Cp interaction while

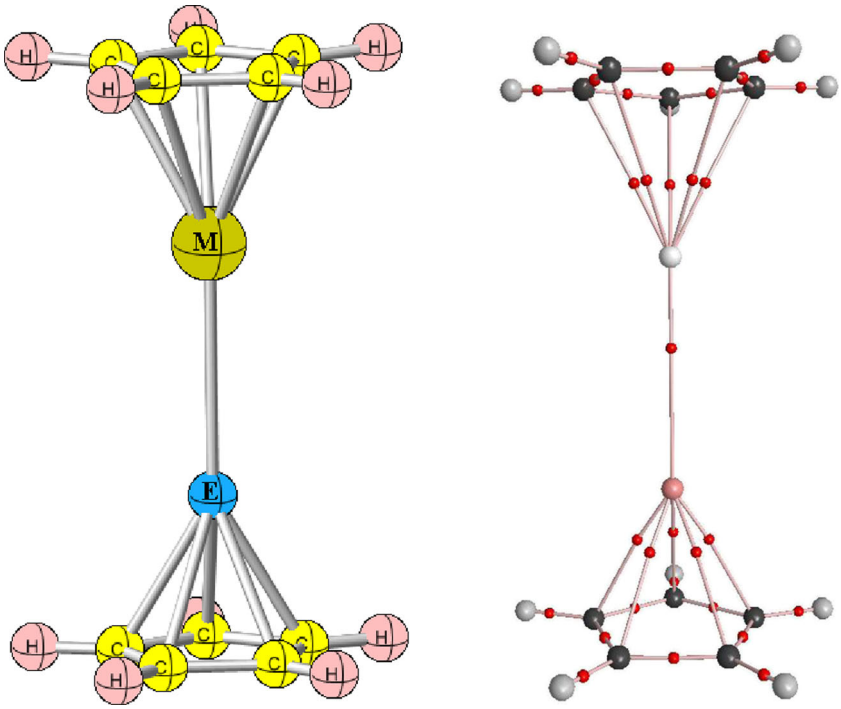

Fig. 1 Geometry and molecular graph of CpE-MCp (E=B, Al, Ga; M=Li, Na, K)

weakening that of M–Cp. The changes will be explained by the NBO. Moreover, as shown in Table 2, the *DI*s between E and C atoms increase after the complexation of ECp and MCp. The increased *DI*s of the E–C bond also prove the enhancing of E–C bonds.

The QTAIM (quantum theory of "atoms in molecules") charges are listed in Table 1. As shown in Table 1, in the studied complexes, the Q(E-Cp) (E = B, Al, and Ga) are positive and Q(M-Cp) (M = Li, Na, and K) are negative. Compared to the neutral systems before complexation, the QTAIM charges mean that the charge transfer is from the M-Cp fragment to the E-Cp fragment.

Comparing the QTAIM charge of E-Cp fragment, it can be seen that the charge transfer decreases in the order E = B, Al, and Ga. This is consistent with the decreasing electronegativity of B, Al, and Ga. That is, the larger electronegative E atom, the greater the charge transfer between E–Cp and M–Cp fragment. The charge transfer tendency is the same as that of $\rho(r_c)$ at the BCP of the E–M bond. This means that the charge transfer plays an important role in the formation of the studied systems.

Other parameters derived from Bader's theory, such as $\nabla^2\rho_b$, H_b and $-G_b/V_b$, can indicate the type of interaction between atoms comprising the bond. As shown in Table 2, The $\nabla^2\rho(r_c)$ and H_c of the M–C bond are positive, and the values of $-G_c/V_c$ are greater than 1, indicating that the M–C interaction has electrostatic characteristics. The $\nabla^2\rho(r_c)$ values of the E–C bond are close to zero, the H_c are negative, and the

Table 1 Calculated geometry parameters of CpE-MCp (E=B, Al, Ga; M=Li, Na, K). *R* Bond length (in Ångstroms), *L* distance (in Ångstroms), *A* bond angle (in degrees), *Q* QTAIM (quantum theory of atoms in molecules) charges

	R(M-E)	R(M-C)	R(E-C)	L(M-Cp Center)	L(E-Cp Center)	A(C-H out of ring plane) M side	A(C-H out of ring plane) E side	Q(E-Cp)	Q(M-Cp)
CpLiBCp	2.261	2.173	1.878	1.807	1.440	0.6(away Li)	4.6(toward B)	−0.037	0.037
CpLiAlCp	2.801	2.135	2.327	1.767	1.990	0.7(away Li)	0.2(toward Al)	−0.028	0.028
CpLiGaCp	2.742	2.406	2.080	1.747	2.080	0.7(away Li)	0.3(away Ga)	−0.006	0.006
CpNaBCp	2.626	2.585	1.881	2.286	1.445	1.7(away Na)	4.4(toward B)	−0.055	0.055
CpNaAlCp	3.172	2.555	2.324	2.252	1.985	1.8 (away Na)	0.1(toward Al)	−0.042	0.042
CpNaGaCp	3.128	2.545	2.404	2.240	2.078	1.8 (away Na)	0.4(away Ga)	−0.034	0.034
CpKBCp	3.164	2.928	1.906	2.668	1.477	1.8(away K)	4.1(toward B)	−0.037	0.037
CpKAlCp	3.782	2.896	2.343	2.633	2.008	1.9(away K)	0.0	−0.030	0.030
CpKGaCp	3.764	2.886	2.428	2.622	2.107	1.9(away K)	0.5(away Ga)	−0.029	0.029

Table 2 Topological properties of bond critical points (BCPs) of various bondings in CpE–MCp (E=B, Al, Ga; M=Li, Na, K). All values in a.u.

Molecules	BCP	$\rho(r_c)$	$\nabla^2\rho(r_c)$	$H(r_c)$	$G(r_c)$	$V(r_c)$	$-G_c/V_c$	DI
CpLi	Li-C	0.028	0.170	0.005	0.037	−0.032	1.151	0.061
CpNa	Na-C	0.018	0.10	0.004	0.021	−0.017	1.217	0.063
CpK	K-C	0.017	0.070	0.002	0.015	−0.013	1.186	0.086
CpB	B-C	0.074	−0.002	−0.038	0.037	−0.075	0.497	0.354
CpAl	Al-C	0.034	0.060	−0.008	0.023	−0.031	0.740	0.230
CpGa	Ga-C	0.037	0.091	−0.005	0.028	−0.032	0.854	0.271
	Li-B	0.023	0.083	0.001	0.020	−0.019	1.036	0.095
CpLiBCp	Li-C	0.024	0.140	0.004	0.031	−0.026	1.167	0.044
	B-C	0.085	0.008	−0.059	0.061	−0.120	0.508	0.286
	Li-Al	0.011	0.030	0.000	0.007	−0.007	1.028	0.071
CpLiAlCp	Li-C	0.026	0.156	0.005	0.034	−0.030	1.159	0.050
	Al-C	0.037	0.092	−0.008	0.031	−0.039	0.792	0.196
	Li-Ga	0.010	0.034	0.001	0.008	−0.007	1.114	0.063
CpLiGaCp	Li-C	0.026	0.160	0.005	0.035	−0.031	1.153	0.051
	Ga-C	0.043	0.102	−0.008	0.033	−0.041	0.812	0.252
	Na-B	0.018	0.064	0.001	0.015	−0.013	1.105	0.123
CpNaBCp	Na-C	0.016	0.086	0.003	0.018	−0.015	1.230	0.045
	B-C	0.085	0.002	−0.058	0.058	−0.116	0.502	0.292
	Na-Al	0.009	0.023	0.000	0.0054	−0.005	1.080	0.092
CpNaAlCp	Na-C	0.017	0.092	0.004	0.020	−0.016	1.225	0.048
	Al-C	0.037	0.093	−0.008	0.032	−0.040	0.792	0.200
	Na-Ga	0.009	0.025	0.001	0.006	−0.005	1.146	0.079
CpNaGaCp	Na-C	0.018	0.095	0.004	0.020	−0.016	1.218	0.049
	Ga-C	0.043	0.102	−0.008	0.033	−0.041	0.812	0.257
	K-B	0.012	0.032	0.001	0.007	−0.006	1.145	0.120
CpKBCp	K-C	0.015	0.062	0.002	0.013	−0.011	1.198	0.067
	B-C	0.082	−0.012	−0.053	0.050	−0.103	0.486	0.295
	K-Al	0.006	0.012	0.000	0.003	−0.002	1.182	0.084
CpKAlCpCpKAlCp	K-C	0.016	0.066	0.002	0.014	−0.012	1.192	0.071
	Al-C	0.037	0.084	−0.008	0.029	−0.037	0.781	0.202
	K-Ga	0.005	0.012	0.001	0.002	−0.002	1.316	0.068
CpKGaCp	K-C	0.017	0.068	0.002	0.015	−0.012	1.187	0.073
	Ga-C	0.041	0.099	−0.007	0.031	−0.038	0.826	0.254

values of $-G_c/V_c$ are smaller than 1.0 but greater than 0.5, indicating that the E–C interaction is partly covalent. The covalent character decreases in the sequence B > Al > Ga.

ELF analysis

Electron localization function (ELF) analysis provides a detailed picture of the bonding, where a set of the core and valence attractors (local maxima), corresponding to atomic cores, lone pairs, and chemical bonds, are obtained. Figure 2 illustrates the topology of the electron localization domains of the E–M bond in CpEMCp. Table 3 collects the basin populations [$N(\Omega_i)$] together with the corresponding variance [$\sigma^2(\Omega_i)$] and relative fluctuations [$\lambda_F(\Omega_i)$] in CpE–MCp (all values in a.u.)

For each compound, there is a valence basin, V(E, M), between two metal atoms, which means that the E–M bonds are conventional two-center bonds. The ELF basin population in the valence basin V(E, Li) is 2.38e, 1.98e and 1.04e; that in V(E, Na) is 2.39, 1.92, and 1.40, and in V(E, K) is 2.44, 1.84 and 1.10 for E = B, Al, Ga, respectively. Moreover, the atom contributions analysis (Table 3) shows that most of the V(E, M) basin population comes from the E atom. These results mean that the E–M bonds are donor–acceptor bonds; the E element is the donor and the M atom is the acceptor. For different E atoms, the changes in the population of V(E, M) are more distinct, decreasing in the sequence E = B > Al > Ga. The influences of the M atom on the population are modest. This means that the E atom determines the bond strength of the E–M bond, whilst the M atom has little

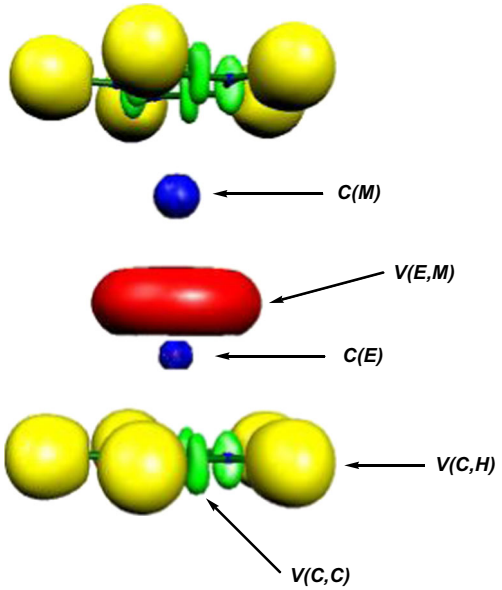

Fig. 2 Three-dimensional (3D) cross section electron localization function (ELF) through the molecules of CpE-MCp

influence on it. The E–M strength decreases in the sequence of E = B, Al, Ga. The populations show that the E–M bonds are double-electron bonds for E = B, decreasing to single-electron bonds for E = Ga.

Furthermore, it is important to observe the relative fluctuations [$\lambda_F(\Omega_i)$] of *V*(E, M). The $\lambda_F(\Omega_i)$ is a good measure of the delocalization extent of a basin and has a value around 0.4 for a well localized bond [49, 50]. As shown in Table 3, the values of $\lambda_F(\Omega_i)$ for V(E, M) increase in the order E = B < Al < Ga. For the B–M bond, the $\lambda_F(\Omega_i)$ is below 0.4, so the B–M bond is well localized. As for E = Al and Ga, the $\lambda_F(\Omega_i)$ values for the Al/Ga–M bond are above 0.65. The Ga–Li bond has the largest $\lambda_F(\Omega_i)$ of 0.86) and the standard deviations [$\sigma^2(\Omega_i)$] are all more than 0.5. The high $\lambda_F(\Omega_i)$ and $\sigma^2(\Omega_i)$ mean that the Al/Ga–M bonds are highly delocalized. The trend revealed by the $\lambda_F(\Omega_i)$ means that the E–M bond changes from being strongly localized to strongly delocalized in the sequence E = B, Al, Ga.

Table 3 also lists the population in the valence basins of E/M and Cp and the atomic contribution of E/M. It can be seen that, in all of the valence basins, the contribution of the M atom to the V(M, C) basin is near to zero. This means that the interactions between the M atoms and the Cp ring are essentially electrostatic. The contribution of the E atom to the V(E, C) basin is larger than that of the M atom, meaning that the E–C bond is partly covalent. This conclusion drawn from ELF is consistent with that from AIM theory.

EDA analysis

To deepen our understanding of the nature of E–M bonding in CpE–MCp, EDA calculation was also carried out. The

Table 3 Electron localization function (ELF) basin populations [$N(\Omega_i)$], variance [$\sigma^2(\Omega_i)$], relative fluctuations [$\lambda_F(\Omega_i)$] in CpE–MCp (E=B, Al, Ga; M=Li, Na, K) (all values in a.u.)

	Ω	N(Ω_i)	Atomic contribution			
			E	M	$\sigma^2(\Omega_i)$	$\lambda_F(\Omega_i)$
CpLiBCp	V(Li, B)	2.38	2.27	0.05	0.86	0.36
	V(Li, C)	14.50		0.07	1.39	0.48
	V(B, C)	13.24	0.22		1.31	0.49
CpLiAlCp	V(Li, Al)	1.00	0.97	0.03	0.65	0.65
		0.98	0.95	0.01	0.64	0.66
	V(Li, C)	14.55		0.11	1.39	0.48
	V(Al, C)	14.46	0.24		1.41	0.49
CpLiGaCp	V(Li, Ga)	0.52	0.52	0.01	0.44	0.86
	V(Li, Ga)	0.52	0.52	0.01	0.44	0.86
	V(Li, C)	14.52		0.09	1.39	0.48
	V(Ga, C)	14.34	0.48		1.41	0.49
CpNaBCp	V(Na, B)	2.39	2.26	0.07	0.85	0.35
	V(Na, C)	14.48		0.04	1.38	0.48
	V(B, C)	13.21	0.22		1.30	0.49
CpNaAlCp	V(Na, Al)	0.79	0.77	0.02	0.57	0.72
		1.13	1.09	0.03	0.68	0.61
	V(Na, C)	14.50		0.11	1.39	0.48
	V(Al, C)	14.47	0.36		1.41	0.49
CpNaGaCp	V(Na, Ga)	0.64	0.63	0.01	0.54	0.84
		0.76	0.76	0.01	0.63	0.83
	V(Na, C)	14.49	0.62		1.39	0.48
	V(Ga, C)	14.36		0.10	1.41	0.49
CpKBCp	V(K, B)	2.44	2.29	0.04	0.87	0.36
	V(K, C)	14.50		0.10	1.39	0.48
	V(B, C)	14.17	0.20		1.39	0.49
CpKAlCp	V(K, Al)	0.68	0.66	0.01	0.52	0.75
		1.16	1.14	0.01	0.70	0.60
	V(K, C)	14.49		0.11	1.39	0.48
	V(Al, C)	14.48	0.38		1.42	0.49
CpKGaCp	V(K, Ga)	1.10	1.09	0.01	0.80	0.73
	V(K, C)	14.49		0.11	1.39	0.48
	V(Ga, C)	14.37	0.44		1.42	0.49

charges and multiplicities are set to 0 and 1 for both CpE and MCp fragments. The overall bond energy ΔE between the fragments is divided into two major components, which can be expressed as $\Delta E = \Delta E_{int} + \Delta E_{prep}$. ΔE_{int} is the instantaneous interaction energy between the two fragments in the molecule. It can be decomposed into three main components. ΔE_{int} is the sum of the Pauli repulsion ΔE_{pauli}, the classical Coulomb interaction ΔE_{elstat} and the orbital interaction term ΔE_{orb}. ΔE_{prep} is the amount of energy required to deform the structures of the free fragments from their equilibrium structure to the geometry that they take up in the molecule. The calculated EDA results are listed in Table 4.

Table 4 Energy decomposition analysis (EDA) results of CpE–MCp (E=B, Al, Ga; M=Li, Na, K) at BLYP/TZP level

	CpLiBCp	CpLiAlCp	CpLiGaCp	CpNaBCp	CpNaAlCp	CpNaGaCp	CpKBCp	CpKAlCp	CpKGaCp
ΔE_{int}	−23.79	−9.72	−4.56	−21.75	−10.39	−4.37	−13.67	−3.41	−1.86
ΔE_{pauli}	14.21	5.04	3.67	12.94	4.53	3.20	8.97	3.28	1.86
ΔE_{elstat} [a]	−30.33 (79.8 %)	−7.31 (49.5 %)	−3.19 (38.8 %)	−29.50 (85.0 %)	−8.31(55.7 %)	−3.74 (49.3 %)	−16.78 (82.3 %)	−4.49 (67.1 %)	−1.91 (51.3 %)
ΔE_{orb} [a]	−7.67 (20.2 %)	−7.45 (50.5 %)	−5.04 (61.2 %)	−5.19 (15.0 %)	−6.61 (44.3 %)	−3.83 (50.5 %)	−3.52 (17.3 %)	−2.20 (32.9 %)	−1.81 (48.7 %)
$\Delta E(A_1)$ [b]	−5.66 (14.9 %)	−6.26 (42.4 %)	−4.18 (50.8 %)	−3.89 (11.2 %)	−5.55 (37.2 %)	−3.23 (42.6 %)	−2.57 (12.7 %)	−1.89 (28.2 %)	−1.47 (39.5 %)
$\Delta E(E_1)$ [b]	−1.85 (4.9 %)	−1.15 (7.8 %)	−0.84 (10.2 %)	−1.17 (3.4 %)	−0.53 (3.5 %)	−0.58 (7.6 %)	−0.88 (4.3 %)	−0.30 (4.5 %)	−0.33 (8.9 %)
$\Delta E(E_2)$ [b]	−0.16 (0.4 %)	−0.04 (0.3 %)	−0.03 (0.2 %)	−0.12 (0.4 %)	−0.03 (0.2 %)	−0.02 (0.3 %)	−0.06 (0.3 %)	−0.01 (0.2 %)	−0.01 (0.3 %)
ΔE_{prep}	2.16	0.84	0.85	1.77	0.86	0.90	0.95	0.48	0.42
$\Delta E(=-D_e)$	−21.63	−8.88	−3.71	−19.98	−9.53	−3.47	−12.72	−2.93	−1.44

[a] Values in parentheses give the percentage contribution to the total attractive interactions $\Delta E_{elstat}+\Delta E_{orb}$

[b] Values in parentheses gives the percentage contribution to the total orbital interactions ΔE_{orb}

The calculated data show that the E–M bond energy, $\Delta E(=-D_e)$, decreases in the order of E = B > Al > Ga for the same M (M = Li, Na, and K), which means that the interaction becomes weaker and weaker in the sequence B > Al > Ga. This sequence is in good agreement with the conclusions drawn from the AIM and ELF results.

The data presented in Table 4 show that the proportion of ΔE_{elstat} in the sum of attractive interactions, i.e., ΔE_{elstat} + $\Delta E_{orb,}$ decreases as E = B > Al > Ga, while ΔE_{orb} shows the reverse trend. For the B–M bond in CpB–MCp, the main energy contributions come from electrostatic interactions, since they are strongly attractive. The proportion of ΔE_{elstat} with respect to the total bonding interactions (ΔE_{elstat} + ΔE_{orb}) is in the range 79.8–85 %. This means that the electrostatic interactions are the dominant attractive interactions between CpB and CpM. For E = Al, the electrostatic interactions in CpAl–MCp are almost equal or slightly larger than the ΔE_{orb} interactions. By contrast, within the CpGa–MCp interactions, the ΔE_{orb} are becomes dominant. These results mean that the predominant B–M bonding is electrostatic. The electrostatic character decreases while the covalent character increases in the sequence B, Al, Ga.

Table 4 also gives the breakdown of the ΔE_{orb} term into the $\Delta E_{\sigma(A1)}$ and $\Delta E_{\pi(E1+E2)}$ contributions. This shows that the σ interactions are important. The relative strength of the π bonding is about 20 % of the ΔE_{orb} values. The B–M bond has the largest π participation compared to the Al–M and Ga–M bond.

NBO analysis

To help visualize the E–M bonding, envelope plots of some relevant natural bond orbitals of the CpB–LiCp are shown in Fig. 3. The molecular orbitals and their occupancy (δ) involving the charge transfer between subsystems, together with the reduction of the second-order perturbation energy (Δ^2E) due to the interaction of donor and acceptor orbitals, as provided by NBO analysis, are collected in Table 5.

From Fig. 3 and Table 5, it can also be seen that the E–M interaction originates from the donor–acceptor interaction. The E atom is the donor and the M atom is the acceptor. The charge is transferred from the lone pair (Lp) or anti-lone pair(Lp*) orbital of the E atom to the Lp* of the M atom. In the formation process of E – M bond, the electrons in anti-lone pair(Lp*) orbital of the E atom decrease. The decreasing electron number in the LP* orbital of the E atom would increase the strengths the E–C bond. For the acceptors, the charge is transferred to the Lp* of M atom, therefore, the strength of M–C decreases. The charge transfer could explain the changes of the $\rho(r_c)$ at BCP. The tendency for charge transfer between CpE and CpM is the same as that of $\rho(r_c)$ at BCP, the larger the charge transfer, the bigger the $\rho(r_c)$. This means that the charge transfer plays an important role in formation of the E–M bond.

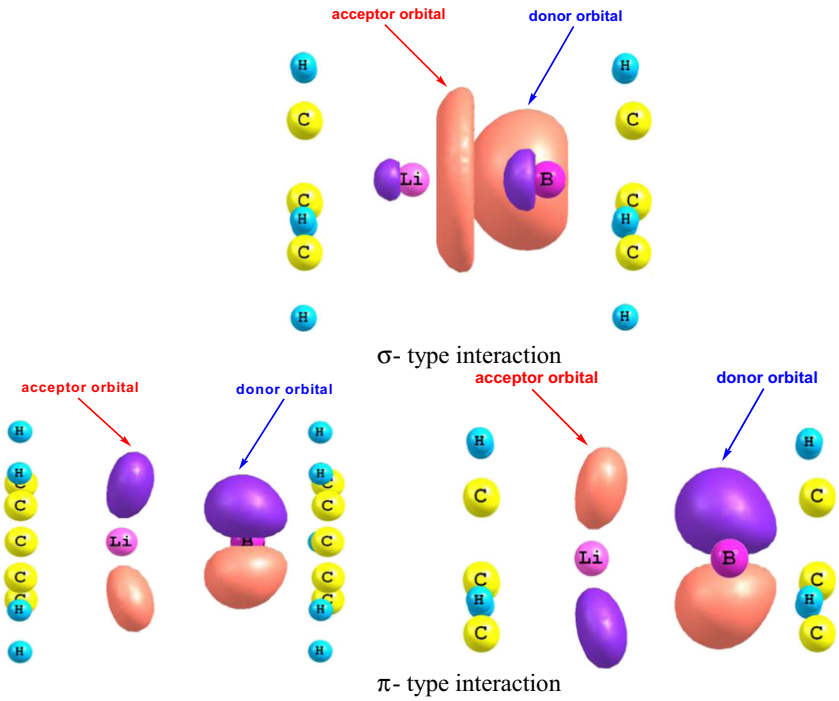

Fig. 3 Isosurface of natural bond orbitals (NBOs) of CpLiBCp

Table 5 The second order energies(kcal mol^{-1}) and atomic orbital contribution based on NBO analysis

Complex	Donor NBO	δ	Acceptor NBO	δ	^2E
CpLiBCp	B lone pair	1.779 ($sp^{0.82}$)	Li anti-lone pair	0.212 ($sp^{1.19}$)	95.87
	B anti-lone pair	0.350 (p)	Li anti-lone pair	0.107 (p)	6.26
		0.350 (p)		0.107 (p)	6.26
CpLiAlCp	Al lone pair	1.7348 (s)	Li anti-lone pair	0.277 ($sp^{1.67}$)	120.35
		0.166 (p)		0.116 (p)	7.41
	Al anti-lone pair	0.166 (p)	Li anti-lone pair	0.116 (p)	7.41
		0.130 ($sp^{8.87}$)		0.277 ($sp^{1.67}$)	101.37
CpLiGaCp	Ga lone pair	1.786 (s)	Li anti-lone pair	0.232 ($sp^{2.34}$)	120.13
		0.188 (p)		0.119 (p)	7.58
	Ga anti-lonepair	0.188 (p)	Li anti-lone pair	0.119 (p)	7.58
		0.124 (p)		0.232 ($sp^{2.34}$)	123.84
CpNaBCp	B lone pair	1.874 ($sp^{0.31}$)	Na anti-lone pair	0.124 ($sp^{0.43}$)	36.98
	B anti-lone pair	0.347 (p)	Na anti-lone pair	0.058 (p)	3.84
		0.347 (p)		0.058 (p)	3.83
CpNaAlCp	Al lone pair	1.838 (s)	Na anti-lone pair	0.171 (sp)	52.22
		0.169 (p)		0.062 (p)	4.14
	Al anti-lone pair	0.169 (p)	Na anti-lone pair	0.062 (p)	4.14
		0.138 ($sp^{7.80}$)		0.171 (sp)	65.84
CpNaGaCp	Ga lone pair	1.881 (s)	Na anti-lone pair	0.131($sp^{1.32}$)	49.98
		0.193 (p)		0.063 (p)	3.98
	Ga anti-lone pair	0.193 (p)	Na anti-lone pair	0.063 (p)	3.98
		0.135 (p)		0.131 ($sp^{1.32}$)	44.8
CpKBCp	B lone pair	1.928 ($sp^{0.26}$)	K anti-lone pair	0.063 ($sp^{0.72}$)	17.55
	B anti-lone pair	0.314 ($sp^{3.59}$)	K anti-lone pair	0.063 ($sp^{0.72}$)	1.71
CpKAlCp	Al lone pair	1.924 (s)	K anti-lone pair	0.080 ($sp^{1.33}$)	20.52
	Al anti-lone pair	0.127 (p)	K anti-lone pair	0.080 ($sp^{1.33}$)	16.72
CpKGaCp	Ga lone pair	1.949 (s)	K anti-lone pair	0.056 ($sp^{1.81}$)	17.55
	Ga anti-lone pair	0.124 (p)	K antibonding	0.056 ($sp^{1.81}$)	15.88

The Lp of B is the sp hybrid orbital, and the component of the p orbital in the sp hybrid orbital decreases in the sequence M = Li > Na > K. The orbital analysis show that the Lp orbitals of Al/Ga atoms are s orbitals. The Lp(E) → Lp*(M) belongs to a σ-type interaction. The Lp* orbitals of both the E and M atoms are p type, so their interactions Lp*(E) → Lp*(M) belong to π-type interactions. From the view of Δ^2E, the larger Δ^2E represents a stronger interaction. Therefore, σ-type interactions play more important roles than the π-type interactions [51].

Conclusions

The nature of the E–M bonds and the E/M–Cp interactions in the donor–acceptor sandwiches CpE–MCp have been calculated and compared using a combination of AIM, ELF and EDA and NBO. The analyses carried out on this work lead to the following main conclusions:

(1) The strength of the donor–acceptor E–M bonds in CpE–MCp is determined mainly by the E atom; the M atom has little influence.
(2) Charge transfer plays an important role in the formation of CpE–MCp.
(3) The E–M strength and electrostatic character decreases in the sequence E = B > Al > Ga. The E–M bonds are double-electron bonds for E = B but decrease to single-electron bonds for E = Ga.
(4) The orbital interaction consists of two types: σ and π. The σ interaction comes from the overlap of the hybrid orbitals and plays a dominant roles in the E–M bond. The π interactions are due to the overlap of the p orbitals of the E and M atoms.
(5) The M–Cp interaction is essentially electrostatic while the E–Cp interaction is partly covalent.

Acknowledgments Thanks to International Science Editing for editing this paper. This work was supported by the National Natural Science Foundation of China (Contract NO. 21102033, 21372062, 21171047, 21373075, 21371045), the Education Department Foundation of Hebei Province (NO. ZD20131053, ZH2012106). The authors would also like to thank Professor Qingzhong Li for providing the ADF2008.1 program.

References

1. Kealy TJ, Pauson P (1951) Nature 168:1039–1040
2. Jutzi P, Burford N (1998) Metallocenes. Wiley, New York
3. Scheirs J, Kaminsky W (2000) Metallocene-based polyolefins, vols 1 and 2. Wiley, Chichester, UK
4. Togni A, Hayashi T (1995) Ferrocenes. Verlach Chemie, Weinheim
5. Jones WD (2005) Inorg Chem 44:4475–4484
6. Jansen G (2000) International Conference on Chemical Bonding: State of the Art in Conceptual Quantum Chemistry. La Colle-sur-Loup: France
7. Resa I, Carmona E, Gutierrez-Puebla E, Monge A (2004) Science 305:1136–1138
8. Xie Y, Schaefer HF III, King RB (2005) J Am Chem Soc 127: 2818–2819
9. Xie Y, Schaefer HF III, Jemmis ED (2005) Chem Phys Lett 402:414–421
10. Xie ZZ, Fang WH (2005) Chem Phys Lett 404:212–216
11. Grirrane A, Resa I, Rodriguez A, Carmona E, Alvarez E, Gutierrez-Puebla E, Monge A, Galindo A, del Rio D, Andersen RA (2007) J Am Chem Soc 129:693–703
12. Li X, Huo S, Sun Z, Zheng SJ, Meng LP (2013) Organometallics 32: 1060–1066
13. Timoshkin AY, Schaefer HF III (2005) Organometallics 24: 3343–3345
14. Gamer MT, Roesky PW, Konchenko SN, Nava P, Ahlriches R (2006) Angew Chem Int Ed 45:4447–4451
15. Merino G, Beltrán HI, Vela A (2006) Inorg Chem 45(3):1091–1095
16. He N, Xie HB, Ding YH (2007) Orgnometallics 26:6839–6843
17. Pauling L, Kamb B (1986) Proc Natl Acad Sci USA 83:3569–3571
18. Bader RFW (1994) Atoms in molecules: a quantum theory. Oxford University Press, Oxford
19. Matta CF, Boyd RJ (2007) The quantum theory of atoms in molecules. From solid state to DNA and drug design. Wiley, Weinheim
20. Silvi B, Savin A (1994) Nature 371:683–686
21. Becke AD, Edgecombe KE (1990) J Chem Phys 92:5397–5403
22. Silvi B (2002) J Mol Struct 614:3–10
23. Savin A, Silvi B, Coionna F (1996) Can J Chem 74:1088–1096
24. Morokuma K (1971) J Chem Phys 55:1236–1245
25. Ziegler T, Rauk A (1977) Theor Chim Acta 46:1–10
26. Coriani S, Haaland A, Helgaker T, Jørgensen P (2006) ChemPhysChem 7:245–249
27. Lee C, Yang W, Parr RG (1988) Phys Rev B 37:785–789
28. Becke AD (1993) J Chem Phys 98:5648
29. Frisch MJ, Trucks GW, Schlegel HB et al (2004) GAUSSIAN 03, Revision D. 02, Gaussian, Inc., Wallingford, CT
30. Krishnan R, Binkley JS, Seeger R, Pople JA (1980) J Chem Phys 72: 650–654
31. Clark T, Chandrasekhar J, Spitznagel GW, Schleyer PR (1983) J Comput Chem 4
32. Popelier P (2000) Atoms in molecules—an introduction. UMIST, Manchester
33. Biegler-König F(2000), AIM 2000, Version 1.0; University of Applied Science: Bielefeld, Germany
34. Keith TA (2010), AIMAll, version 10.05.04, see http://aim.tkgristmill.com/
35. Feixas F, Matito E, Duran M, Solà M, Silvi B (2010) J Chem Theory Comput 6:2736–2742
36. Noury S, Krokidis X, Fuster F, Silvi B (1999) J Comput Chem 23: 597–604
37. Matito E, Silvi B, Duran M, Sola M (2006) J Chem Phys 125:24301
38. Lu T, Chen F (2012) J Comput Chem 33:580–592
39. ADF2008.01, SCM, Theoretical Chemistry, Vrije Universiteit, Amsterdam, The Netherlands. Available from: http://www.scm.com
40. van Lenthe E, Baerends EJ, Snijers JG (1994) J Chem Phys 101:9783
41. Reed AE, Curtiss LA, Weinhold F (1988) Chem Rev 88:899–926
42. Weinhold F (1997) J Mol Struct THEOCHEM 398:181–197
43. Kar T, Ángyán JG, Sannigrahi AB (2000) J Phys Chem A 104: 9953–9963
44. Firme CL, Antunes OAC, Esteves PM (2009) Chem Phys Lett 468: 129–133
45. Bader RFW, Matta CF (2001) Inorg Chem 40:5603
46. Wang YG, Matta, C, Werstiuk, NH(2003) J Comp Chem 1720–1729

47. Bianchi R, Gervasio G, Marabello D (2000) Inorg Chem 39: 2360–2366
48. Cremer D, Kraka E (1984) Angew Chem Int Ed Engl 23:627–628
49. Noury S, Colonna F, Savin A, Silvi B (1998) J Mol Struct 450:59–68
50. Llusar R, Beltrán A, Andrés J, Fuster F, Silvi B (2001) J Phys Chem A 105:9460–9466
51. Glendening ED, Landis CR, Weinhold F (2012) WIRES Comput Mol Sci 2:1–42